Liquid-Phase Synthesis of Doped Nanoparticles: Colloids of Luminescing $LaPO_4$:Eu and $CePO_4$:Tb Particles with a Narrow Particle Size Distribution

K. Riwotzki, H. Meyssamy, A. Kornowski, and M. Haase*

Institut für Physikalische Chemie, Universität Hamburg, Bundesstrasse 45, D-20146 Hamburg, Germany

Received: October 6, 1999

Nanocrystals of $LaPO_4$:Eu and $CePO_4$:Tb with a mean particle size of 5 nm and a narrow size distribution have been prepared by reacting the corresponding metal chlorides, phosphoric acid, and a base at 200 °C in tris(ethylhexyl) phosphate. Highly crystalline material was obtained as confirmed by X-ray powder diffraction measurements and high-resolution transmission electron microscopy. Successful doping with europium was evident from the splitting and the intensity pattern of the luminescence lines. Luminescence lifetime measurements were used to confirm doping and energy transfer in both materials. Colloidal solutions of $CePO_4$:Tb exhibit an overall luminescence quantum yield of 16%.

Introduction

The liquid-phase synthesis in high-boiling coordinating solvents is a versatile method for preparing a variety of colloidal nanocrystals. Well-known examples for this approach are the synthesis of cadmium chalcogenide nanoclusters[1] and TiO_2 nanoclusters[2] in trioctylphosphine oxide (TOPO), of InP nanoclusters[3,4] and InAs nanoclusters[5] in trioctylphosphine (TOP), and of ZnSe nanoclusters[6] in hexadecylamine. Since the boiling points of these coordinating solvents are high, the synthesis can be performed at temperatures between 200 and 300 °C, resulting in particles with excellent crystallinity. Size-selective precipitation methods have been developed to separate the raw product into fractions with very narrow particle size distributions.[1,4,5]

Elevated temperatures have been found useful also in the liquid-phase synthesis of doped nanoparticles. Temperatures between 200 and 270 °C have been applied, for instance, in the hydrothermal synthesis (i.e., wet chemical synthesis at high temperatures in an autoclave) of blue-colored colloids of *n*-doped SnO_2:Sb[7] and of lanthanide-doped nanoparticles of YVO_4[8] and $LaPO_4$.[9] Successful incorporation of the dopant ions into the host has been confirmed by EXAFS measurements[10−12] or, in case of doping with europium, by analyzing the crystal field splitting of the f−f transitions.[8,9,13,14] In the wet chemical synthesis of colloidal ZnS:Mn[15−20] and CdS:Mn,[21−24] doping has been achieved even at room temperature. Attempts to prepare CdS:Er[25] nanoparticles at room-temperature, however, resulted in deposition of a large fraction of the dopant ions onto the outer surface of the nanoparticles. In the case of SnO_2:Eu xerogels,[26] heating of the dry nanocrystalline powder to temperatures above 300 °C was found to be necessary to achieve incorporation of the europium ions.

In this paper we present the synthesis of lanthanide-doped phosphates in the coordinating solvent tris(ethylhexyl) phosphate. While attempts using TOPO as the solvent failed, the synthesis in tris(ethylhexyl) phosphate yielded colloids of highly crystalline nanoparticles and a narrow particle size distribution.

Experimental Section

Synthesis. For the synthesis of $LaPO_4$:Eu nanoparticles 490 mg (5.0 mmol) of crystalline H_3PO_4 and 6.5 mL (15 mmol) of trioctylamine are dissolved in 30 mL of tris(ethylhexyl) phosphate (Fluka) and combined with a solution containing 1.76 g of $La(NO_3)_3 \cdot 7H_2O$ (4.75 mmol) and 92 mg of $EuCl_3 \cdot 6H_2O$ (0.25 mmol) in 50 mL of tris(ethylhexyl) phosphate. Using standard Schlenk line techniques the colorless transparent liquid is degassed under vacuum and subsequently heated to 200 °C under nitrogen for 16 h. During heating, some of the phosphoric acid ester is cleaved and the boiling point of the colloid decreases to about 180 °C.

Powders of the nanocrystals are obtained by adding methanol to the transparent colloid, resulting in precipitation of the nanocrystals. The latter are separated by centrifugation, washed twice with methanol, and dried. Colloids have been obtained also by redispersing 50 mg of the powder in 10 mL of 2-propanol containing a few drops of a 25 wt % solution of tetrabutylammonium hydroxide in methanol (Fluka) and passing the dispersion through a 0.14 μm filter.

$CePO_4$:Tb nanoparticles are prepared similarly by reacting a solution of 1.58 g (4.25 mmol) of $Ce(NO_3)_3 \cdot 6H_2O$ and 280 mg of $Tb(NO_3)_3 \cdot 5H_2O$ (0.75 mmol) in tris(ethylhexyl) phosphate with a solution of 6.5 mL (15 mmol) of trioctylamine and 490 mg (5.0 mmol) of crystalline H_3PO_4 in tris(ethylhexyl) phosphate. To minimize oxidation to Ce^{4+}, the metal chlorides were dissolved under nitrogen.

Anhydrous metal chlorides dissolve equally well if they are free of oxychlorides and may be used instead of the hydrated chlorides. Precipitation of the nanocrystals, however, is often less efficient in this case. The solvent tris(ethylhexyl) phosphate may be replaced by the lower boiling tributyl phosphate.

Characterization. Transmission electron micrographs of the samples were acquired on a Philips CM 300 UT electron microscope (300 kV acceleration voltage) equipped with a CCD camera (Gatan, model 694).

A Philips X'pert system and Philips Rietveld plus software[27] were used to measure and to analyze the X-ray diffraction pattern of powder samples, respectively.

Dilute colloidal solutions of nanoparticles were placed in 1 cm cuvettes, and their absorption and luminescence spectra were measured using a Lambda 40 spectrometer (Perkin-Elmer) and a Spex Fluoromax 2 spectrometer, respectively.

The room-temperature quantum yields of the scatter-free colloidal solutions were determined by comparing the emission

10.1021/jp993581r CCC: $19.00
Published on Web 03/10/2000

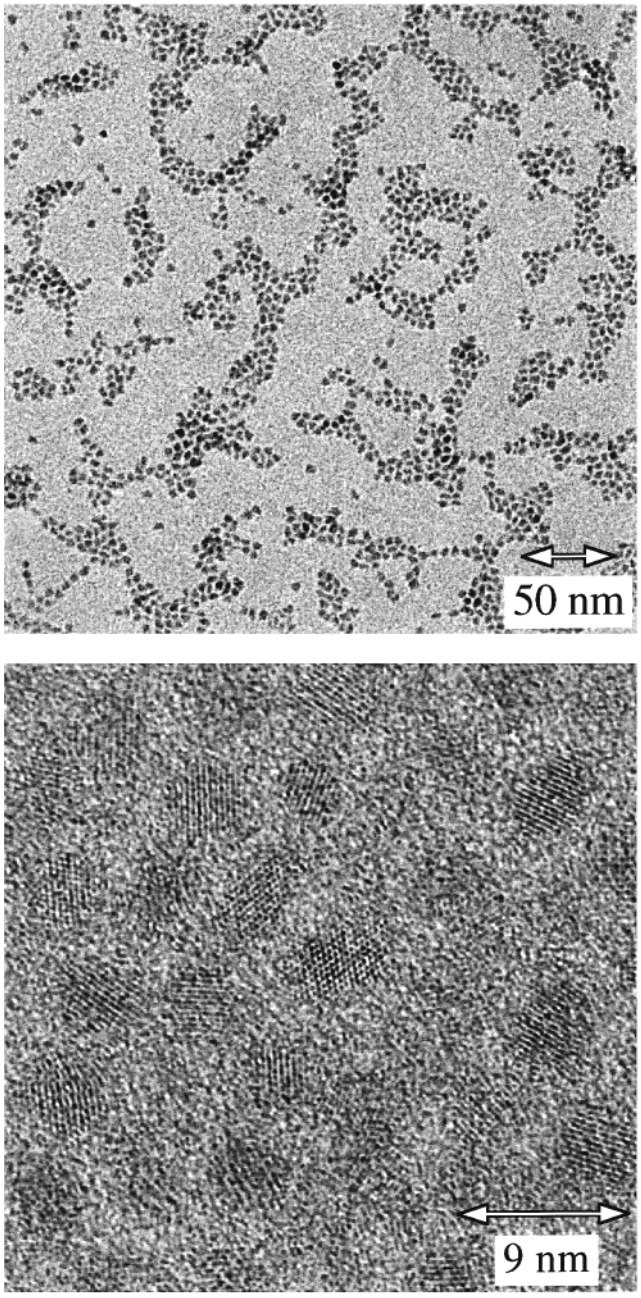

Figure 1. Top part: TEM of $LaPO_4$:Eu nanoparticles. Bottom part: HRTEM showing individual nanoparticles of $LaPO_4$:Eu.

of the colloidal solution with the emission of a solution of rhodamine 6G (Lambda Physics, laser grade; in spectroscopic grade ethanol) of identical optical density at the excitation wavelength.

Luminescence decay curves were measured by exciting the colloids at 266 nm with 15 ns laser pulses of low intensity (Forth harmonics of a Nd:YAG laser, Spectron Laser Systems, model SL804F10) and recording the time-dependent luminescence intensity at a preselected wavelength. For these measurements a double monochromator (Schoeffel, model EM 200), a Hamamatsu R928 photomultiplier, and a digital oscilloscope (Hewlett-Packard, model 54522 A) were used.

Results and Discussion

A transmission electron micrograph (TEM) displaying the very narrow size distribution of the colloids is given in the top part of Figure 1. The image shows well-separated $LaPO_4$:Eu nanoparticles ranging in size from 4 to 5 nm. The high-resolution transmission electron micrograph (HRTEM) given in the bottom part of the figure displays lattice fringes for most particles, indicating highly crystalline material. Similar micrographs are obtained for $CePO_4$:Tb nanoparticles.

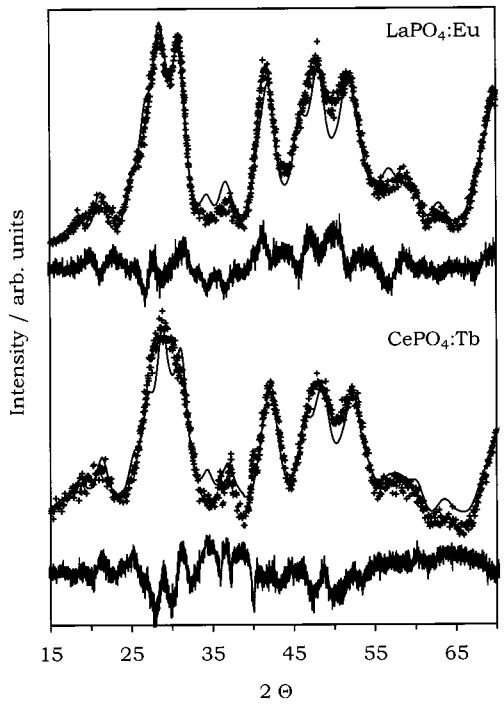

Figure 2. Top part: X-ray powder diffraction data (+), Rietveld fit (solid line through data points), and difference curve of $LaPO_4$:Eu nanocrystals (solid line below data points). Bottom part: same as above for $CePO_4$:Tb nanocrystals.

TABLE 1: Results of the Rietveld Fits Given in Figure 2

	$LaPO_4$:Eu	$CePO_4$:Tb
space group	*P*121/*n*1 (14)	*P*121/*n*1 (14)
unit cell params		
a (Å)	6.830	6.830
b (Å)	7.072	7.082
c (Å)	6.502	6.502
α (deg)	90	90
β (deg)	103.3	103.3
γ (deg)	90	90
particle size: $\langle D \rangle_V$ (nm)	4.5	5.0

Figure 2 shows the X-ray diffraction (XRD) data, Rietveld simulation[28] of the data, and the difference curve between the XRD data and the Rietveld fit. For clarity, only every third data point is given in the figure. In both data sets the background was approximated by a straight horizontal line. Since the signal-to-noise ratio of the XRD data is much smaller than for bulk materials, a Rietveld refinement is not possible. Nevertheless, the Rietveld simulations show that both XRD patterns are in accord with a nanocrystalline monazite phase. The numerical values used in the Rietveld fits (Table 1) indicate that the space group and the dimensions of the unit cells are the same as for the corresponding monazite bulk materials. The Rietveld fits yield volume-averaged mean particle sizes of 4.5 and 5.0 nm for $LaPO_4$:Eu and $CePO_4$:Tb, respectively, well in accordance with the electron micrographs. However, we cannot deduce the strain in the crystal lattice of our nanoparticles from the XRD data, since even large values for strain cause a much weaker broadening of the XRD peaks than the small particle size does.

In Figure 3 the luminescence line spectrum of a colloidal solution of $LaPO_4$:Eu is shown. Vertical lines mark the spectral

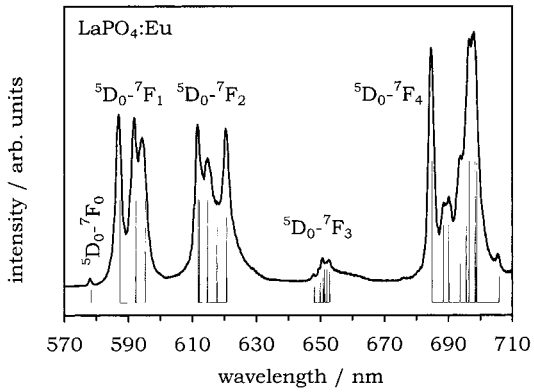

Figure 3. Luminescence spectrum of a colloidal solution of nanocrystalline $LaPO_4$:Eu (λ_{ex} = 260 nm). Main lines of the emission spectrum are due to transitions from the $^5D_0$ level of Eu^{3+}. Vertical lines indicate transitions from the $^5D_0$ level observed in bulk material.

position of luminescence lines of the corresponding bulk material.[29] The luminescence lines correspond to transitions between f-electron levels of the europium dopant ions. The position and the intensity of these transitions are affected by the symmetry and the strength of the crystal field at the europium site, enabling the use of europium ions as a structural probe of dopant site symmetry.[30] In bulk $LaPO_4$:Eu the europium site has C_1 symmetry.[31] The transition energies of europium in $LaPO_4$:Eu have been calculated and are in good agreement with the spectral positions actually observed in the bulk material.[29] Figure 3 shows clearly that the positions of the luminescence lines of the nanocrystals are identical to those of the bulk material, indicating that the local crystal environment of the dopant is the same in both materials. The intensity pattern of the luminescence lines given in Figure 3 is practically identical to the one observed for hydrothermally prepared 50 nm $LaPO_4$:Eu particles.[9] For the latter, it was shown that the intensity pattern changes slightly if the nanoparticles are heated (sintered) to 1300 K, whereas the line positions are not altered. Moreover, low-temperature luminescence spectra (15 K) of the annealed particles reveal that heating at 1300 K decreases the width of the luminescence lines. These results possibly indicate that several C_1 symmetry sites coexist in the nanomaterials and that the number and occupation of these sites change upon heating to high temperatures. In fact, three different europium sites have been identified in bulk $LaPO_4$:Eu[29] by site-selective-spectroscopy techniques.

Successful doping is also evident from the luminescence excitation spectrum of $LaPO_4$:Eu nanoparticles shown in the top part of Figure 4. The spectrum consists of a strong band below 300 nm and several sharp lines of weaker intensity and is practically identical to the spectrum reported for bulk $LaPO_4$:Eu.[32] The broad absorption below 300 nm is due to an oxygen-to-europium charge-transfer transition,[32] whereas the sharp lines correspond to direct excitation of the europium ground state into higher excited states of the europium f-electrons. Since the spectrum has been recorded at room temperature, transitions from the $^7F_1$ state located 264 cm^{-1} above the $^7F_0$ ground state are also observed (bottom part of Figure 4). Again, the transition energies and the splitting pattern of these lines are in accord with the theoretical model[29] given for the bulk material (vertical lines).

The luminescence quantum yield of the colloidal solution of $LaPO_4$:Eu is less than 10% upon excitation at 277 nm, i.e., excitation of the charge-transfer transition. An exact value cannot be given yet, since the oxygen-to-europium charge-transfer band and the f−f transitions have low extinction coefficients, making it difficult to accurately determine the absorption of the colloid at the excitation wavelength.

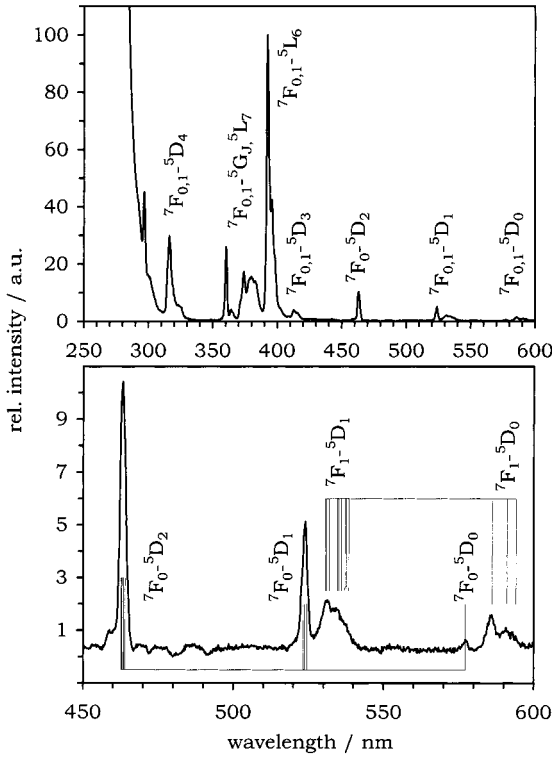

Figure 4. Top part: luminescence excitation spectrum (λ_{em} = 614 nm) of a colloidal solution of $LaPO_4$:Eu nanoparticles. Bottom part: comparison of the transition energies of several lines of the luminescence excitation spectrum with theoretical values (vertical lines) given for the bulk material.

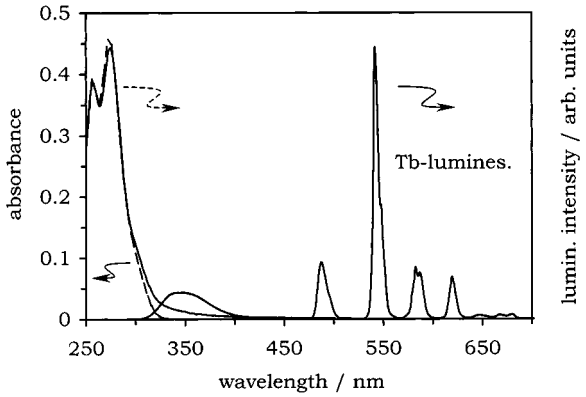

Figure 5. UV−vis absorption spectrum (solid line between 250 and 400 nm), luminescence spectrum (solid line between 300 and 700 nm), and luminescence excitation spectrum (broken line) of a colloidal solution of $CePO_4$:Tb.

In contrast to $LaPO_4$:Eu, the absorption spectrum of $CePO_4$:Tb nanoparticles exhibits a strong band in the UV due to the optically allowed 4f−5d transition of cerium. The absorption spectrum of colloidal $CePO_4$:Tb is shown in Figure 5 together with the luminescence spectrum and the luminescence excitation spectrum. The cerium absorption band is much stronger than the weak oxygen-to-europium charge-transfer transition of $LaPO_4$:Eu. In contrast to europium and terbium, cerium displays no line spectrum as its excited d-electron state exhibits strong electron−phonon coupling. Since the excited state is strongly split by the crystal field, the absorption consists of two overlapping bands.[33] The cerium absorption band shows a weak

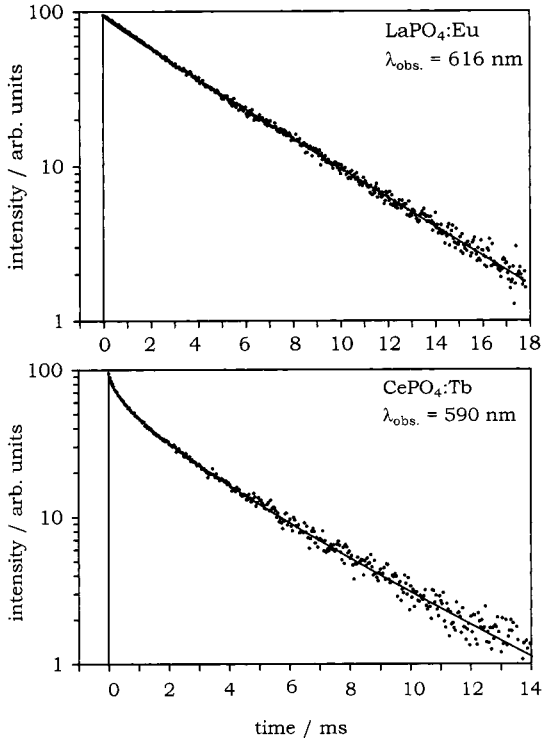

Figure 6. Luminescence decay curves (data points) of colloidal solutions of $LaPO_4$:Eu nanocrystals (top part) and $CePO_4$:Tb nanocrystals (bottom part) (λ_{ex} = 266 nm, t_{ex} = 15 ns). Solid lines: fits according to the model given in the text.

extension from about 300 to 450 nm, which is caused by the presence of a small amount of Ce^{4+}.[32]

The luminescence spectrum in Figure 5 shows the typical line spectrum of the terbium $^5D_4-^7F_J$ transitions between 450 and 700 nm.[34] Since in the case of terbium not only the ^7F_J states but also the $^5D_4$ state is split into several sublevels by the crystal field, each peak in the spectrum consists of a large number of unresolved lines. Due to the high Ce^{3+} concentration in the particles, the cerium luminescence is not completely quenched by terbium and is observed in the luminescence spectrum as an additional broad peak between 300 and 400 nm. The colloidal solutions of $CePO_4$:Tb exhibit a quantum yield of 16% if the emission of cerium is included and 11% if the emission of terbium is considered only.

The luminescence excitation spectrum, recorded at the main terbium line at 542 nm, is almost identical to the absorption spectrum. Obviously, the excitation energy is transferred from Ce^{3+} to Tb^{3+}, as is known from the bulk material.[33] As expected, the absorption caused by Ce^{4+} is not observed in the luminescence excitation spectrum since energy transfer from Ce^{4+} to terbium is impossible.

Figure 6 shows the luminescence decay curves of europium and terbium in nanocrystalline $LaPO_4$:Eu and $CePO_4$:Tb, respectively. As expected, the luminescence lifetimes are in the range of milliseconds. However, only nanocrystalline $LaPO_4$:Eu shows an almost single-exponential luminescence decay as is observed for both bulk materials, whereas the luminescence of nanocrystalline $CePO_4$:Tb strongly deviates from single-exponential behavior.

This type of nonexponential luminescence kinetics is frequently observed in materials where energy transfer from the excited state of the luminescing ions to impurity ions takes place, leading to luminescence quenching.[35] Luminescence quenching of this kind has been shown to occur, for instance, in bulk $LaPO_4$:Tb codoped with rare-earth ions such as Nd^{3+}, Ho^{3+}, Pr^{3+}, or Er^{3+}.[32] Pure $LaPO_4$:Tb shows a single-exponential luminescence decay with a lifetime of 3.2 ms. Both the luminescence kinetics and the lifetime are reported to remain unchanged even at high terbium concentrations, indicating the absence of energy migration over the Tb^{3+} ions. In the presence of Nd^{3+}, Ho^{3+}, Pr^{3+}, or Er^{3+}, however, the Tb luminescence is quenched via electric-dipole interaction of the terbium ions with the codopant, resulting in a nonexponential luminescence decay, similar to the one shown in the lower part of Figure 6. Assuming dipole−dipole interaction between the luminescing and the quenching ions, a statistical distribution of both ions in the lattice, and the absence of energy migration over the luminescing ions, the luminescence decay may be described approximately by[36]

$$I(t) = I_0 \exp\left(-\frac{t}{\tau_R} - 2C\left(\frac{t}{\tau_R}\right)^{1/2}\right) \qquad C = \frac{2}{3}\pi^{3/2} n_q R_0^{\,3}$$

where τ_R is the intrinsic decay time of the excited ion, n_q is the concentration of quencher ions, i.e., the number per m^3. In the case of dipole−dipole interaction between luminescing and quenching ions the range parameter R_0 is defined by $R_0^6 = \tau_R R^6 W(R)$, where $W(R)$ is the transition probability for energy transfer and R corresponds to the separation of two interacting ions. Note that $W(R)$ itself is proportional to R^{-6}.

Since the model given above describes a statistical distribution of ions in bulk material, it assumes that any value between zero and infinity is realized for the separation R of two interacting ions. In our samples, however, the limited size of the nanoparticles allows only for separations smaller than about 50 Å. Nevertheless, we expect the model to give an approximate description of the data, since due to the R^{-6} dependence of the dipole−dipole mechanism the interaction between ions separated by more than 10 Å is very weak. By using values of $\tau_R = 4.8$ ms and $C = 0.13$ for $LaPO_4$:Eu and values of $\tau_R = 5.8$ ms and $C = 1.28$ for $CePO_4$:Tb, we are able to describe the experimental curves quite well (Figure 6). The value of C is small for $LaPO_4$:Eu, as expected for a material showing an almost single-exponential luminescence decay. Obviously, energy transfer from the excited europium level is weak. The intrinsic luminescence lifetime τ_R deduced from the model is somewhat larger than the value of $\tau_R \approx 3.2$ ms reported for bulk $LaPO_4$:Eu.[29]

The high value of C in the case of $CePO_4$:Tb reflects its strongly nonexponential luminescence decay (Figure 6) and shows that energy transfer to quenching ions is much more pronounced than in $LaPO_4$:Eu. This may be caused by the presence of Ce^{4+} ions in $CePO_4$:Tb (see above), which are known to quench the luminescence of terbium.

The value of C may be used to calculate to what extent the quantum yield is reduced by energy transfer from the luminescing ions to impurity ions: The total number of photons emitted by the dopant is proportional to the area under the luminescence decay curve. Integrating the expression given above yields

$$\int_0^\infty I(t)\,\mathrm{d}t = I_0\tau_R(1 - \pi^{1/2} C \exp(C^2)\,\mathrm{erfc}(C))$$

In the absence of quenching ions, i.e., if $n_q = 0$ and, hence, $C = 0$, the luminescence decays single-exponentially and the integrated intensity is proportional to $I_0 \cdot \tau_R$. Consequently, if the luminescence quantum yield ϕ is equal to unity in the absence of energy transfer, a quantum yield of

$$\phi = 1 - \pi^{1/2} C \exp(C^2)\,\mathrm{erfc}(C)$$

is expected if quenching is active. Using the values for C determined above, quantum yields of 89% and 38% are calculated for nanocrystalline $LaPO_4$:Eu and $CePO_4$:Tb, respectively. These values are much higher than the quantum yields observed upon excitation of the host. This indicates that the excited state of the host is depleted by energy transfer not only to the luminescence centers but also to centers where radiationless recombination occurs. Likely centers for the latter may be the same quencher ions to which energy from the luminescing ions is transferred or surface states of the nanoparticles. If radiationless recombination takes place mainly at the particle surface, the quantum yield may be improved by modifying the surface of the particles or by epitactically growing a shell of inert material around each nanoparticle ("core−shell particles"). These concepts have been successfully applied to semiconductor nanoparticles and have increased their luminescence quantum yields to values between 30% and more than 60%.[37−44]

Summary

The liquid-phase synthesis in high-boiling coordinating solvents proves to be a useful method for preparing doped colloidal nanocrystals. Colloids of $LaPO_4$:Eu and $CePO_4$:Tb with a mean particle size of 5 nm and a narrow size distribution have been prepared at 200 °C. Both nanomaterials exhibit the monazite phase, i.e., the same phase observed for bulk materials prepared at much higher temperatures. Doping of the nanoclusters with lanthanide ions has been successful, as is evident from their luminescence spectra. In particular, the Eu^{3+} emission can be used to show that the symmetry of the dopant site is the same as in the bulk material. The luminescence decay curves of both materials show deviations from single-exponential kinetics. The deviation is considerably more pronounced for $CePO_4$:Tb than for $LaPO_4$:Eu, the former of which contains Ce^{4+} ions. The nonexponential behavior can be explained by energy transfer from the excited state of the luminescing ions to ions where radiationless recombination occurs. The low quantum yields observed upon excitation of the host indicate that energy transfer to the luminescence centers is not the only channel by which the excited state of the host lattice is depleted. A second mechanism may involve energy transfer from the host to either quenching ions or, in view of the small particle size, the particle surface where radiationless recombination occurs.

Acknowledgment. We thank J. Ludwig and Dr. Klaska from the Mineralogisch-Petrographisches Institut of the University of Hamburg for the measurement of the XRD spectra. We greatly acknowledge funding of this project by the German Science Foundation (DFG).

References and Notes

(1) Murray, C. B.; Norris, D. J.; Bawendi, M. G. *J. Am. Chem. Soc.* **1993**, *115*, 8706.
(2) Trentler, T. J.; Denler, T. E.; Bertone, J. F.; Agrawal, A.; Colvin, V. L. *J. Am. Chem. Soc.* **1999**, *121*, 1613.
(3) Micic, O. I.; Curtis, C. J.; Jones, K. K.; Sprague, J. R.; Nozik, A. J. *J. Phys. Chem*. **1994**, *98*, 4966.
(4) Guzelian, A. A.; Katari, J. E. B.; Kadavanich, A. V.; Banin, U.; Hamad, K.; Juban, E.; Alivisatos, A. P.; Wolters, R. H.; Arnold, C. C.; Heath, J. R. *J. Phys. Chem*. **1996**, *100*, 7212.
(5) Guzelian, A. A.; Banin, U.; Kadavanich, A. V.; Peng, X.; Alivisatos, A. P. *Appl. Phys. Lett*. **1996**, *69*, 1432.
(6) Hines, M. A.; Guyot-Sionnest, P. *J. Phys. Chem. B* **1998**, *102*, 3655.
(7) Nütz, T.; zum Felde, U.; Haase, M. *J. Chem. Phys.* **1999**, *110*, 12142.
(8) Riwotzki, K.; Haase, M. *J. Phys. Chem. B* **1998**, *102*, 10129.
(9) Meyssamy, H.; Riwotzki, K.; Kornowski, A.; Naused, S.; Haase, M. *Adv. Mater*. **1999**, *11*, 840.
(10) Soo, Y. L.; Ming, Z. H.; Huang, S. W.; Kao, Y. H.; Bhargava, R. N.; Gallagher, D. *Phys. Rev. B: Condens. Matter* **1994**, *50* (11), 7602.
(11) Soo, Y. L.; Huang, S. W.; Ming, Z. H.; Kao, Y. H.; Smith, G. C.; Goldburt, E.; Hodel, R.; Kulkarni, B.; Veliadis, J. V. D.; Bhargava, R. N. *J. Appl. Phys.* **1998**, *83*, 5404.
(12) Rockenberger, J.; zum Felde, U.; Tischer, M.; Tröger, L.; Haase, M.; Weller, H. *J. Chem. Phys*., submitted for publication.
(13) Bihari, B.; Eilers, H.; Tissue, B. M. *J. Lumin.* **1997**, *75*, 1.
(14) Williams, D. K.; Bihari, B.; Tissue, B. M.; McHale, J. M. *J. Phys. Chem. B.* **1998**, *102*, 916.
(15) Becker, W. G.; Bard, A. J. *J. Phys. Chem*. **1983**, *87*, 4888.
(16) Gallagher, D.; Heady, W. E.; Racz, J. M.; Bhargava, R. N. *J. Cryst. Growth* **1994**, *138*, 970.
(17) Bhargava, R. N.; Gallagher, D.; Hong, X.; Nurmikko, A. *Phys. Rev. Lett*. **1994**, *72*, 416.
(18) Bhargava, R. N. *J. Lumin.* **1996**, *70* (1−6), 85.
(19) Sooklal, K.; Cullum, B. S.; Angel, S. M.; Murphy, C. J. *J. Phys. Chem.* **1996**, *100*, 4551.
(20) Bol, A. A.; Meijerink, A. *Phys. Rev. B: Condens. Matter* **1998**, *58* (24), R15998.
(21) Counio, G.; Esnouf, S.; Gacoin, T.; Boilot, J.-P. *J. Phys. Chem.* **1996**, *100*, 20021.
(22) Levy, L.; Hochepied, J. F.; Pileni, M. P. *J. Phys. Chem*. **1996**, *100*, 18322.
(23) Levy, L.; Feltin, F.; Ingert, D.; Pileni, M. P. *J. Phys. Chem. B* **1997**, *101*, 9153.
(24) Counio, G.; Gacoin, T.; Boilot, J.-P. *J. Phys. Chem. B* **1998**, *102*, 5257.
(25) Schmidt, T.; Müller, G.; Spanhel, L.; Kerkel, K.; Forchel, A. *Chem. Mater*. **1998**, *10*, 65.
(26) Brito, G. E. S.; Rebeiro, S. J. L.; Briois, V.; Dexpert-Ghys, J.; Santilli, C. V.; Pulcinelli, S. H. *J. Sol.-Gel Sci. Technol*. **1997**, *8*, 261.
(27) Fischer, R. X.; Lengauer, C.; Tillmanns, E.; Ensink, R. J.; Reiss, C. A.; Fantner, E. J. *Mater. Sci. Forum* **1993**, *287*, 133−136.
(28) Young, R. A. *The Rietveld Method*; Oxford University Press: Oxford, 1993.
(29) Dewxpert-Ghys, J.; Mauricot, R.; Faucher, M. D. *J. Lumin.* **1996**, *69*, 203.
(30) Peacock, R. D. *Struct. Bonding* **1975**, *22*, 83.
(31) Ropp, R. C. *J. Electrochem. Soc.* **1968**, *115* (8) 841.
(32) van Schaik, W.; Lizzo, S.; Smit, W.; Blasse, G. *J. Electrochem. Soc.* **1993**, *140* (1), 216.
(33) Bourcet, J.-C.; Fong, F. K. *J. Chem. Phys*. **1974**, *60*, 34.
(34) Hashimoto, N.; Takada, Y.; Sato, K.; Ibuki, S. *J. Lumin*. **1991**, *48*, *49*, 893.
(35) Huber, D. L. *Phys. Rev. B* **1979**, *20*, 2307.
(36) Watts, R. K. In *Optical Properties of Ions in Solids*; Di Bartolo, B., Ed.; Plenum Press: New York, 1975; p 307.
(37) Spanhel, L.; Haase, M.; Weller, H.; Henglein, A. *J. Am. Chem. Soc.* **1987**, *109*, 5649.
(38) Kontan, A. R.; Hull, R.; Opila, R. L.; Bawendi, M. G.; Steigerwald, M. L.; Carroll, P. J.; Brus, L. E. *J. Am. Chem. Soc.* **1990**, *112*, 1327.
(39) Hoener, C. F.; Allan, K. A.; Bard, A. J.; Campion, A.; Fox, M. A.; Mallouk, T. E.; Webber, S. E.; White, J. M. *J. Phys. Chem.* **1992**, *96*, 3812.
(40) Danek, M.; Jensen, K. F.; Murray, C. B.; Bawendi, M. G. *Chem. Mater*. **1996**, *8*, 173.
(41) Hines, M. A.; Guyot-Sionnest, P. *J. Phys. Chem.* **1996**, *100*, 468.
(42) Micic, O. I.; Sprague, J. R.; Lu, Z.; Nozik, A. J. *Appl. Phys. Lett.* **1996**, *68*, 3150.
(43) Peng, X.; Schlamp, M. C.; Kadavanich, A. V.; Alivisatos, A. P. *J. Am. Chem. Soc.* **1997**, *119*, 7019.
(44) Dabbousi, B. O.; Rodriguez-Viejo, J.; Mikulec, F. V.; Heine, J. R.; Mattoussi, H.; Ober, R.; Jensen, K. F.; Bawendi, M. G. *J. Phys. Chem. B* **1997**, *101*, 9463.